Polarized Infrared Study of Hybrid Langmuir−Blodgett Monolayers Containing Clay Mineral Nanoparticles

R. H. A. Ras,[†] C. T. Johnston,*[,‡] E. I. Franses,[§] R. Ramaekers,[∥] G. Maes,[∥] P. Foubert,[⊥] F. C. De Schryver,[⊥] and R. A. Schoonheydt[†]

Centrum voor Oppervlaktechemie en Katalyse, K.U.Leuven, Kasteelpark Arenberg 23, B-3001 Leuven, Belgium, Birck Nanotechnology Center, 915 W. State Street, Purdue University, West Lafayette, Indiana 47907-2054, School of Chemical Engineering, 1283 Chemical Engineering Building, Purdue University, West Lafayette, Indiana 47907-1283, Fysische en Analytische Chemie, Departement Scheikunde, K.U.Leuven, Celestijnenlaan 200F, B-3001 Leuven, Belgium, and Afdeling Fotochemie en Spectroscopie, Departement Scheikunde, K.U.Leuven, Celestijnenlaan 200F, B-3001 Leuven, Belgium

Received November 1, 2002. In Final Form: February 28, 2003

Hybrid clay-organic monolayers prepared using the Langmuir−Blodgett (LB) method are examined by polarized infrared attenuated total reflection spectroscopy (ATR), polarized grazing angle infrared reflection absorption spectroscopy (IRRAS), and atomic force microscopy (AFM). These spectra represent the first reported IR spectra of clay monolayers functionalized with cationic surfactants. The intensities of the ν(Si−O) bands of SapCa-1 saponite and SWy-1 montmorillonite on both Ge and ZnSe substrates were analyzed quantitatively using the thin film approximation. The measured intensity on both substrates corresponds to the calculated intensity of one clay layer (0.96 nm), indicating that a monolayer of clay was formed on ZnSe as well as on Ge. In the case of saponite, a trioctahedral smectite, the ν(OH) band at 3680 cm^{-1} and the out-of-plane ν(Si−O) band at 1063 cm^{-1} show dichroic ratios of 0.33 and 0.23, respectively, consistent with the nearly perpendicular orientation of these bonds in the film. For SWy-1, a dioctahedral smectite, the ν(OH) bands have a dichroic ratio of slightly higher than 1.0, indicating that the structural OH groups are oriented more within the 001 plane. The dichroic ratios of the δ(OH) bands (AlAlOH, FeAlOH, and MgAlOH bending) show small differences representing subtle changes in mutual orientation of the hydroxyl groups. Similar to saponite, the out-of-plane ν(Si−O) of SWy-1 is highly oriented with a dichroic ratio of 0.12. Infrared reflection absorption spectra show even more pronounced dichroic ratios of the ν(Si−O) bands. From the polarized IR spectra and AFM, it has been confirmed that the clay particles are highly oriented in the LB monolayer.

Introduction

Nanostructured organic−inorganic hybrid ultrathin films have gained widespread interest because of their potential use in a number of diverse technological applications. Organic materials impart flexibility and versatility whereas the inorganic particles provide structural stability and can have unique conducting, semiconducting, or dielectric properties. Clay minerals are inorganic, sheetlike particles that can be incorporated into ultrathin hybrid films. Langmuir−Blodgett (LB)[1−9] and self-assembly[10−19] are excellent methods to construct ultrathin hybrid clay films since they operate at ambient conditions and allow control of thickness and structure in monolayers and in multilayers that are assembled layer-by-layer. While self-assembly is a fast and simple method, LB films generally possess a higher degree of organization.

The LB method has been used to fabricate ultrathin hybrid films consisting of layers of a swelling 2:1 phyllosilicate clay (smectite) and amphiphilic cations.[1−9] Initial work on the spreading of surfactant−smectite complexes over a water subphase in a LB trough resulted in the formation of multilayered clay−organic cation complexes consisting of 5−13 intercalated sheets of clay. Recently, hybrid LB clay films consisting of a *single* layer of the smectite−amphiphile complex have been reported[4−6] for alkylammonium cations ($C_nH_{2n+1}NH_3^+$, $n = 4-18$) with a natural saponite, a trioctahedral 2:1 phyllosilicate. When

* To whom correspondence may be addressed.
[†] Centrum voor Oppervlaktechemie en Katalyse, K.U.Leuven.
[‡] Birck Nanotechnology Center, Purdue University.
[§] School of Chemical Engineering, Purdue University.
[∥] Fysische en Analytische Chemie, Departement Scheikunde, K.U.Leuven.
[⊥] Afdeling Fotochemie en Spectroscopie, Departement Scheikunde, K.U.Leuven.

(1) Inukai, K.; Hotta, Y.; Taniguchi, M.; Tomura, S.; Yamagishi, A. *J. Chem. Soc., Chem. Commun.* **1994**, 959.
(2) Kotov, N. A.; Meldrum, F. C.; Fendler, J. H.; Tombacz, E.; Dekany, I. *Langmuir* **1994**, *10*, 3797.
(3) Inukai, K.; Hotta, Y.; Tomura, S.; Takahashi, M.; Yamagishi, A. *Langmuir* **2000**, *16*, 7679.
(4) Umemura, Y.; Yamagishi, A.; Schoonheydt, R.; Persoons, A.; De Schryver, F. *Thin Solid Films* **2001**, *388*, 5.
(5) Umemura, Y.; Yamagishi, A.; Schoonheydt, R.; Persoons, A.; De Schryver, F. *Langmuir* **2001**, *17*, 449.
(6) Takahashi, S.; Taniguchi, M.; Omote, K.; Wakabayashi, N.; Tanaka, R.; Yamagishi, A. *Chem. Phys. Lett.* **2002**, *352*, 213.
(7) Umemura, Y.; Yamagishi, A.; Schoonheydt, R.; Persoons, A.; De Schryver, F. *J. Am. Chem. Soc.* **2002**, *124*, 992.
(8) Umemura, Y. *J. Phys. Chem. B* **2002**, *106*, 11168.
(9) Schoonheydt, R. A. *Clays Clay Miner.* **2002**, *50*, 411.
(10) van Duffel, B.; Schoonheydt, R. A.; Grim, C. P. M.; De Schryver, F. C. *Langmuir* **1999**, *15*, 7520.
(11) van Duffel, B.; Verbiest, T.; Van Elshocht, S.; Persoons, A.; De Schryver, F. C.; Schoonheydt, R. A. *Langmuir* **2001**, *17*, 1243.
(12) Kleinfeld, E. R.; Ferguson, G. S. *Science* **1994**, *265*, 370.
(13) Ferguson, G. S.; Kleinfeld, E. R. *Adv. Mater.* **1995**, *7*, 414.
(14) Kleinfeld, E. R.; Ferguson, G. S. *Chem. Mater.* **1995**, *7*, 2327.
(15) Kotov, N. A.; et al. *J. Am. Chem. Soc.* **1997**, *119*, 6821.
(16) Hotta, Y.; Inukai, K.; Taniguchi, M.; Yamagishi, A. *J. Colloid Interface Sci.* **1997**, *188*, 404.
(17) Glinel, K.; Laschewsky, A.; Jonas, A. M. *Macromolecules* **2001**, *34*, 5267.
(18) Kim, D. W.; Blumstein, A.; Kumar, J.; Tripathy, S. K. *Chem. Mater.* **2001**, *13*, 2742.
(19) Ariga, K.; Lvov, Y.; Ichinose, I.; Kunitake, T. *Appl. Clay Sci.* **1999**, *15*, 137.

10.1021/la026786r CCC: $25.00
Published on Web 04/11/2003

a solution of the alkylammonium salt in chloroform is spread over a dilute aqueous smectite suspension in the LB trough to form a spread monolayer, the clay particles adsorb on the surfactant layer forming a floating hybrid monolayer of the smectite−surfactant complex.

Evidence for the formation of monolayers of the smectite−amphiphilic complex has included surface pressure−molecular area ($\pi-a$) isotherm measurements,[3−5] atomic force microscopy (AFM),[3−5] IR spectroscopy,[3,5] and grazing angle in-plane X-ray diffraction.[6] The surface pressure−molecular area ($\pi-a$) isotherm measurements were strongly influenced by the presence of the clay with the lift-off area of the cation being shifted to progressively larger areas with increasing clay concentration. AFM studies of hybrid LB clay films have shown that clay particles cover ∼90% of the available surface.[5,6] AFM-derived thickness measurements have shown the films to be between 1 and 5 nm thick. In a combined AFM-XRD (X-ray diffraction) study of the saponite−octadecylammonium complex,[6] the thickness of the hybrid films was reported to be between 3.0 and 3.6 nm, consistent with the sum of the thickness of one elementary smectite platelet (0.96 nm) and the length of the octadecylammonium cation (∼2.5 nm). Additionally, in-plane XRD and specular X-ray reflection measurements show indirect evidence consistent with a single layer of the hybrid film.[6] Transmission FTIR spectroscopy has been used to study the ν(CH) region of alkyl chains of multilayered hybrid LB clay films.[3,5] A linear increase in the intensities of the ν(CH) bands as a function of the number of dipping cycles has been observed, showing that multiple layers could be built up. Recently, we have examined the vibrational properties of smectite in aqueous suspension using in situ ATR and ordinary FTIR transmission methods.[20] Polarized ATR-FTIR methods were used to study the thickness and orientation of thin films coating ZnSe internal reflection elements (IREs) from aqueous suspension. On the basis of the dichroic ratio of the *in-plane* and *out-of-plane* ν-(Si−O) vibrations, it was concluded that the thin smectite films were highly oriented on the surface of the IRE. The absorption coefficient of the ν(Si−O) bands was found to be 3.6×10^4 cm^{-1}, corresponding to an absorbance value of 0.0015 au per fundamental layer (0.96 nm) of smectite. On the basis of this quite large infrared absorption coefficient, IR detection of single layers of smectite was considered possible and is the subject of the present investigation. Although IR methods have been used to study hybrid LB clay films, their use has been restricted to a study of the ν(CH) region. Polarized ATR-FTIR or IRRAS spectra of hybrid LB clay films have not been reported previously. The purpose of this study is to examine the IR spectra of the ν(Si−O) and ν(OH) regions of the smectite and to determine the thickness of the hybrid clay films based on intensities of the ATR-FTIR spectra. These spectroscopic data of single smectite layers pave the way for spectroscopy of single clay particles. Such data can be the basis for theoretical studies of elementary clay mineral platelets within the frame of molecular mechanics or ab initio or density functional theory quantum-mechanical methods. Ultimately it may be possible to calculate the macroscopic properties of clay minerals from experimental data of single elementary sheets.

Materials and Methods

The clays used in this study were the SapCa-1 saponite (Ballarat) and SWy-1 montmorillonite (Wyoming) specimens obtained from the Source Clays Repository of the Clay Minerals Society. The clays were Na^+ saturated by repeated (three times) exchange with 1 M NaCl solutions followed by dialysis with water until a negative Cl^- test was obtained using $AgNO_3$. The particle size fractions between 0.5 and 2.0 μm for SapCa-1 and the <0.5 μm for SWy-1 were obtained by centrifugation and freeze-drying of a salt-free, Na-exchanged clay suspension. The SapCa-1 and SWy-1 clays were stored in dark and have water content of respectively 7% and 4% as determined by thermogravimetric analysis. The amphiphilic molecules *N*,*N*′-dioctadecyl oxacarbocyanine perchlorate (OXA18; Fluka), octadecyl rhodamine B chloride (RhB18; Molecular Probes), dimethyl dioctadecylammonium bromide (Acros), and 1-hexadecylpyridinium chloride (Fluka) were used as received. *N*,*N*′-Dioctadecyl thiacyanine (THIA18, gift from M. Vanderauweraer) was prepared according to Sondermann[21] and was recrystallized three times from acetic acid. These organic salts were dissolved in HPLC grade chloroform to prepare solutions of 10^{-3} mol/dm^3.

LB films were prepared on a NIMA Technology model 611 LB trough at a temperature of 23 °C. A dilute saponite clay suspension (50 mg clay/dm^3) stirred for 24 h in Milli-Q water was used as the subphase. A microsyringe was used to spread between 25 and 200 μL of the amphiphiles dissolved in chloroform over the subphase. After ∼15 min, the film was compressed at a rate of 30 cm^2 min^{-1} or 12.5 Å^2 molecule^{-1} min^{-1}. Films were deposited in upstroke (lifting speed of 5 mm min^{-1}) on ZnSe and Ge IREs at surface pressures ranging from 3 to 20 mN m^{-1}. The substrates were cleaned prior to each deposition by gently rubbing with a paper tissue soaked in methanol.

The cast clay film was prepared by pipetting a dilute clay suspension of the Na-exchanged saponite on a ZnSe window. The film was allowed to dry under ambient conditions. The self-supporting clay film was prepared according to Johnston et al.[22] The cast and self-supporting films were measured in transmission IR using a Perkin-Elmer model 2000 GX spectrometer. The IREs were ZnSe and Ge 45° trapezoidal-shaped crystals (SPT, Harrick) (50 mm × 20 mm × 2 mm) with 25 internal reflections and were measured in a vertical ATR cell using a Bruker IFS66/S FTIR spectrometer. Because the IRE was not covered with film where it was attached to the dipper, there are only 24 active reflections. Infrared reflection absorption spectra of the films on ZnSe and Ge IREs were measured on a Nicolet Nexus spectrometer using a Specac monolayer/grazing angle accessory (19650) at grazing angle of 80°. Polarized infrared reflection absorption and attenuated total reflectance (ATR)-FTIR spectra were obtained using a wire-grid polarizer. All FTIR spectrometers were equipped with a liquid nitrogen cooled MCT detector and a KBr beam splitter. A total of 256 individual scans were signal averaged using an optical resolution of 2 cm^{-1}. Spectra were analyzed with Grams/32 AI version 6.00 software.

The ν(Si−O) absorption coefficient of the Na-saponite clay mineral was determined using a similar procedure as reported recently.[20] The method consists of deposition of 1−2 mL aliquots of a dilute aqueous suspension of Na-saponite on the surface of a round ZnSe window (50 mm diameter × 2 mm thick) and allowing the film to dry. The cast clay film outside of a square region in the center of the window (20 mm × 20 mm) was removed. The mass of the clay deposit was measured to within the nearest 1×10^{-5} g, and the IR transmission spectrum of the cast film was measured.

AFM measurements were performed with the PicoSPM (Molecular Imaging), with the SPM1000 control electronics (RHK), operating in contact AFM mode. The contact mode cantilevers with reflective coating and ultrasharp silicon tips (CSC21A, MikroMasch) have a force constant of 0.21 N/m (value supplied by manufacturer). Scanning was performed at a typical line speed of 0.5 Hz, with a 512 pixel resolution. Images are leveled by horizontal background subtraction, and the color scales are adjusted for optimal representation.

Results and Discussion

AFM Image of Clay−Surfactant LB Film Deposited on ZnSe IRE. The AFM topography image of SWy-RhB18 LB film deposited on ZnSe IRE at 5 mN m^{-1} (Figure 1) shows that the IRE is largely covered with sheetlike particles of irregular shape. The root-mean-square value

(20) Johnston, C. T.; Premachandra, G. S. *Langmuir* **2001**, *17*, 3712.

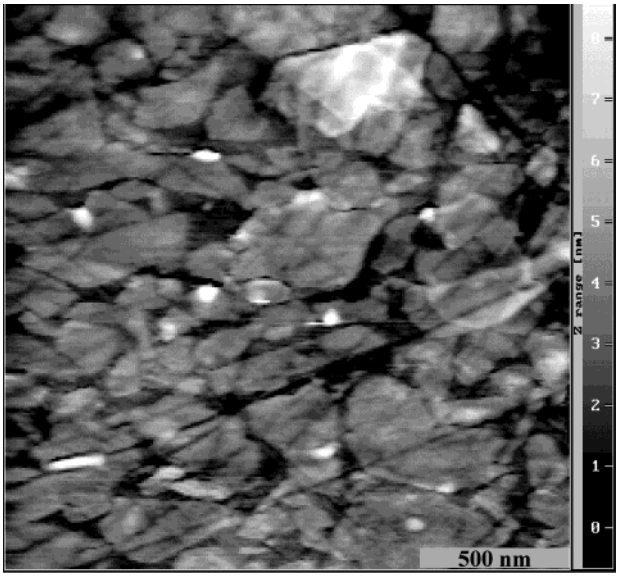

Figure 1. AFM topography image of SWy-RhB18 LB film deposited on ZnSe IRE at 5 mN m^{-1}. The grayscale bar at the right represents the height corresponding to each pixel. The length of the bar in the bottom right corner represents 500 nm.

of the topography, which can be a measure for average surface roughness, is calculated to be 1.69 nm. The lateral dimensions of the particles range from several tens of nanometers up to more than 500 nm. The thickness of the particles ranges from 1.5 nm up to 3.4 nm. This corresponds to a single clay layer (0.96 nm) and a surfactant layer. An error can be introduced in the thickness measurements because the surface of ZnSe IRE is not extremely flat and contains some scratches. When a clay particle is located on top of such a scratch, the sheet is deformed such that the scratch can still be seen in the topography image. Single clay particles are shown to be flexible enough to adapt their shape to the underlying surface. In the upper part of the image, three clay particles are on top of each other, although the major part of the film consists of single layered clay.

Comparison of ATR-FTIR Spectra of Hybrid LB Clay Films to Transmission IR Spectra of Self-Supporting and Cast Films. The ATR-FTIR spectrum of a saponite−THIA18 LB film (Figure 2a) is compared with the transmission IR spectra of a self-supporting clay film (Figure 2c) and a cast clay film on a ZnSe window (Figure 2b). The thickness of the self-supporting film is ∼10 μm,[22] and the thickness of the cast film is ∼2 μm. The thickness of clay films can be determined based on the peak absorbance value in the ν(Si−O) region as has been shown by Johnston et al.[20] Expanded portions of these spectra in the ν(OH) and ν(Si−O) regions are shown in the inset boxes in Figure 2, where each spectrum is scaled separately. In the ν(OH) region, the broad bands at 3580, 3460, and 3250 cm^{-1} in the spectra of self-supporting and cast films are due to sorbed water on these thicker clay films[20,23−29] In the spectrum of the LB film, the ν(OH) band is well resolved at 3680 cm^{-1} and the ν(OH) bands of water are not detected (Figure 2, inset ((OH) region).

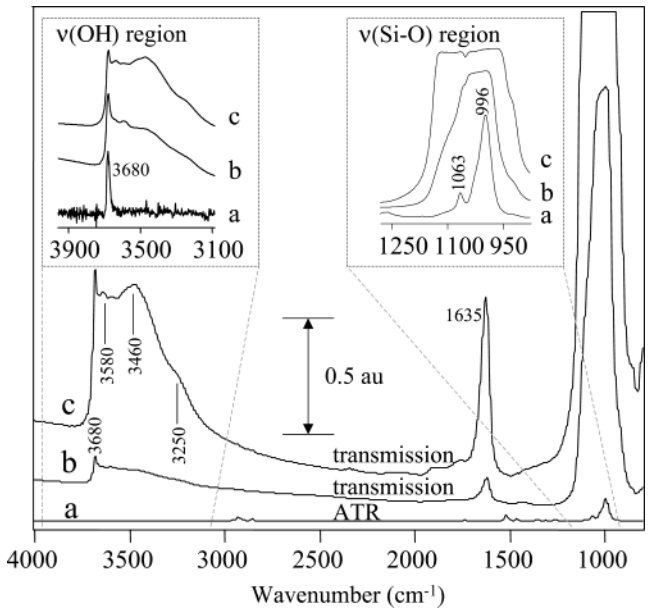

Figure 2. Comparison of unpolarized transmission IR spectra of sodium saponite clay to the p-polarized ATR spectrum of saponite-THIA18 LB film: (a) p-polarized ATR-FTIR spectrum of hybrid saponite-THIA18 LB film; (b) unpolarized transmission IR spectrum of a film cast from aqueous suspension, (c) unpolarized transmission IR spectrum of a self-supporting clay film, sample (b) and (c) contain some residual water (inset ν-(OH) region) expanded scale showing the region from 3900 to 3100 cm^{-1}, (inset ν(Si−O) region) expanded scale showing the region from 1250 to 900 cm^{-1}. See Table 1 for band assignments.

Hybrid LB clay films were prepared using the surfactants *N*,*N*′-dioctadecyl oxacarbocyanine, octadecyl rhodamine B, dimethyl dioctadecylammonium, 1-hexadecylpyridinium, and *N*,*N*′-dioctadecyl thiacyanine (THIA18), and similar spectra in the ν(OH) region were obtained. The δ(HOH) bending band of water at 1635 cm^{-1} is present in the spectra of the self-supporting and cast films and is absent in the spectra of the LB films. The lack of water in these spectra indicates that the organic cations have replaced essentially all of the Na^+ ions originally on the saponite.

Similarly, the ν(Si−O) bands of the LB hybrid clay film are considerably better resolved compared with the spectra of the self-supporting and cast films (Figure 2, inset ν-(Si−O) region). The most intense ν(Si−O) band at 996 cm^{-1} (Figure 2, Table 1) corresponds to the *in-plane* ν-(Si−O) mode (e_1^1 vibration), and the less intense band at 1063 cm^{-1} corresponds to the *out-of-plane* ν(Si−O) band (a_1^1 vibration).[30] These band positions compare favorably with values of 1005−1014 cm^{-1} for the *in-plane* ν(Si−O) band and a poorly resolved shoulder between 1044 and 1056 cm^{-1} observed in oriented films tilted at non-normal incidence.[31]

In this study, the absorption coefficient α_{max} of the ν-(Si−O) band at 996 cm^{-1} of saponite was determined to be 3.5 × 10^4 cm^{-1}, in close agreement with the value of 3.6 × 10^4 cm^{-1} reported for SWy-1. These absorption

(21) Sondermann, J. *Liebigs Ann. Chem.* **1971**, *749*, 183.
(22) Johnston, C. T.; Sposito, G.; Erickson, C. *Clays Clay Miner.* **1992**, *40*, 722.
(23) Farmer, V. C.; Russell, J. D. *Trans. Faraday Soc.* **1971**, *67*, 2737.
(24) Xu, W.; Johnston, C. T.; Parker, P.; Agnew, S. F. *Clays Clay Miner.* **2000**, *48*, 120.
(25) Skipper, N. T.; Sposito, G.; Chang, F. R. C. *Clays Clay Miner.* **1995**, *43*, 294.
(26) Chang, F. R. C.; Skipper, N. T.; Sposito, G. *Langmuir* **1995**, *11*, 2734.
(27) Skipper, N. T.; Smalley, M. V.; Williams, G. D.; Soper, A. K.; Thompson, C. H. *J. Phys. Chem.* **1995**, *99*, 14201.
(28) Chang, F. R. C.; Skipper, N. T.; Sposito, G. *Langmuir* **1998**, *14*, 1201.
(29) Karaborni, S.; Smit, B.; Heidug, W.; Urai, J.; vanOort, E. *Science* **1996**, *271*, 1102.
(30) Farmer, V. C. *The infrared spectra of minerals*; Farmer, V. C., Ed.; Mineral Society: London, 1974; p 331.
(31) Margulies, L.; Rozen, H.; Banin, A. *Clays Clay Miner.* **1988**, *36*, 476.

Table 1. Band Assignment, Position, Width, Height, Dichroic Ratio of the Clay Bands in the Polarized ATR-FTIR Spectra Obtained Using a ZnSe IRE with an Angle of Incidence of 45°[a]

SapCa-1 (Ballarat saponite−trioctahedral)

band assignments (ref 30 and footnotes *b* and *c*)	position, cm^{-1}	width, cm^{-1}	height A_s	height A_p	dichroic ratio $R = A_s/A_p$	n_{ZnSe} (ref 38)	n_{clay} (*d*)	γ, deg
ν(OH) of structural hydroxyl groups	3680	19.3	0.0014	0.0042	0.33	2.439		
ν(Si-O)	1086	18.5	0.0035	0.0029	1.21	2.411	0.74	62
out-of-plane ν(Si-O)	1063	20.5	0.0088	0.0402	0.23	2.409	0.687	19.5
ν(Si-O)	1027	23.7	0.0171	0.0170	1.01	2.407	1.29	62
in-plane ν(Si-O)	996	36.5	0.1197	0.1042	1.11	2.406	2.006	74

SWy-1 (Wyoming montmorillonite−dioctahedral)

band assignments	position, cm^{-1}	width, cm^{-1}	height A_s	height A_p	dichroic ratio $R = A_s/A_p$	n_{ZnSe}	n_{clay}	γ, deg
ν(OH) of structural hydroxyl groups	3628	59.2	0.0067	0.0062	1.08	2.439		
ν(Si-O) (longitudal mode)	1116	28.8	0.0140	0.0147	0.95	2.412	0.844	57
out-of-plane ν(Si-O)	1085	33.2	0.0049	0.0393	0.12	2.411	0.606	12
in-plane ν(Si-O)	1047	23.0	0.0815	0.0668	1.22	2.409	1.864	90
in-plane ν(Si-O)	1024	35.2	0.0954	0.0858	1.11	2.407	2.365	80
δ(OH) of the AlAlOH group	919	29.5	0.0094	0.0079	1.18	2.400	1.759	90
δ(OH) of the FeAlOH group	885	21.6	0.0048	0.0042	1.13	2.397	1.693	80
δ(OH) of the MgAlOH group	846	23.9	0.0045	0.0034	1.31	2.394	1.645	90

[a] The average tilt angle γ of the IR transition dipole moments was calculated[43] using the listed values of refractive index of ZnSe and clay. The symbols ν and δ denote stretching and bending vibrational modes, respectively. [b] Ishii, M.; Shimanouchi, T.; Nakahira, M. *Inorg. Chim. Acta* **1967**, *1*, 387. [c] Madejova, J.; Komadel, P. *Clays Clay Miner.* **2001**, *49*, 410. [d] Roush, T.; Pollack, J.; Orenberg, J. *Icarus* **1991**, *94*, 191.

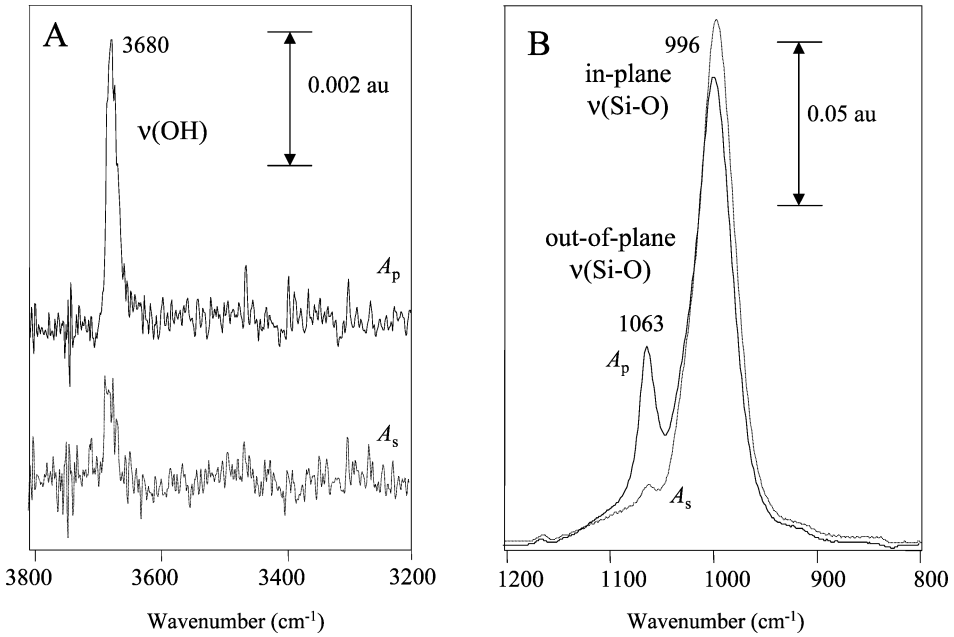

Figure 3. Polarized ATR-FTIR spectra of a hybrid LB film of SapCa-1 clay with THIA18 deposited on ZnSe at a surface pressure of 5 mN/m: (A) ν(OH) region; (B) ν(Si−O) region. See Table 1 for peak assignments.

coefficients compare to α_{max} values ranging from 1.3 to 2.5 $\times 10^4$ cm^{-1} obtained from amorphous Si−O materials.[32] The higher α_{max} values for the smectites are attributed to the preferential orientation of the film which provides maximum interaction of the *in-plane* ν(Si−O) bonds with the incident IR radiation.

Polarized ATR-FTIR Spectra of Hybrid Clay Films. The ν(OH) and ν(Si−O) regions of the polarized ATR-FTIR spectra of the hybrid saponite-THIA18 LB film are shown in Figure 3. Whereas in the A_p polarization, both *out-of-plane* and *in-plane* vibrations are observed, mainly *in-plane* vibrations are active in the A_s polarization.[33] In both regions, large polarization effects are evident with the 3680 and 1063 cm^{-1} bands having dichroic ratios $R = A_s/A_p$ of <0.35. In the ν(OH) region, the 3680 cm^{-1} band has a dichroic ratio of 0.33 consistent with the orientation of the OH groups normal to the 001 plane (Figure 3A).[34−36] Saponite is a trioctahedral smectite with all octahedral positions occupied. The most favorable position for the structural OH group is normal to the clay sheet. Similar polarization behavior is observed with the 1063 cm^{-1} band (Figure 3B), assigned to the out-of-plane ν(Si−O) vibration (a_1^1 vibration).[30] The average dichroic ratio of this band is 0.23 in agreement with a recent ATR-

(32) Trchova, M.; Zemek, J.; Jurek, K. *J. Appl. Phys.* **1997**, *82*, 3519.

(33) Fringeli, U. P. *Internal Reflection Spectroscopy. Theory and Applications*; Mirabella, F. M., Ed.; Marcel Dekker: New York, 1993; p 255.

(34) Giese, R. F. *Clays Clay Miner.* **1979**, 27, 213.

(35) Suquet, J.; Prost, R.; Pezerat, H. *Clay Miner.* **1977**, *12*, 113.

(36) R. Prost, *Proceedings of the International Clay Conference, 1975, Mexico City, Mexico*; Bailey, S. W., Ed.; Applied Publishing Ltd.: Wilmette, IL, 1975; p 351.

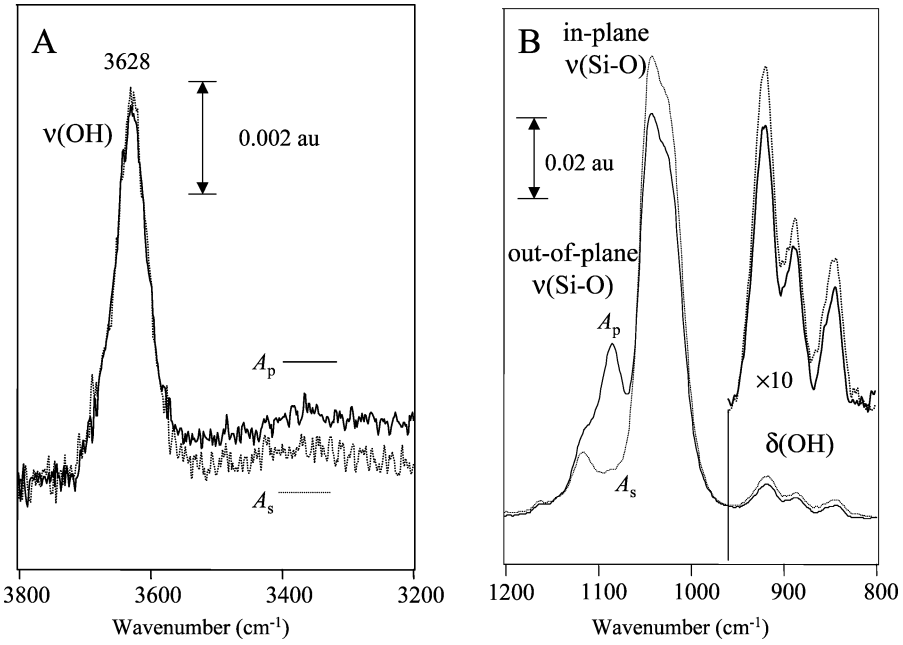

Figure 4. Polarized ATR-FTIR spectra of a hybrid LB film of SWy-1 clay with THIA18 deposited on ZnSe at a surface pressure of 5 mN/m: (A) ν(OH) region; (B) ν(Si−O) + δ(OH) region. See Table 1 for peak assignments.

FTIR study of dioctahedral smectites in aqueous suspension.[20] The main ν(Si−O) vibration at 996 cm^{-1} has a dichroic ratio of 1.11 resulting from the in-plane orientation of the Si−O group. The average tilt angle of the Si−O bonds projected on the 001 plane is ∼20 ± 5°.

The ν(OH) and ν(Si−O) regions of the polarized ATR-FTIR spectra of the hybrid SWy-THIA18 LB film are shown in Figure 4. SWy-1 montmorillonite is a dioctahedral smectite of which two of the three octahedral sites are occupied with Al^{3+}, Fe^{3+}, and Mg^{2+} and the structural hydroxyl lies nearly in the 001 plane (tilted 16° with respect to the 001 plane).[30] The dichroic ratio of the ν(OH) band at 3628 cm^{-1} is slightly higher than 1, which is an indication for an orientation of the hydroxyl rather in the plane of the layer (Figure 4A). Montmorillonite is a dioctahedral clay with 1/3 of the octahedral sites vacant. The most favorable position of the structural OH group is toward this vacancy. The absence of ν(OH) bands in the 3550−3200 cm^{-1} region again demonstrates that no sorbed water is present.

The ν(Si−O) vibrations of SWy-1 (Figure 4B) have a similar polarization behavior as for those of SapCa-1 (Figure 3B). The out-of-plane ν(Si−O) at 1085 cm^{-1} has a dichroic ratio $R = 0.12$, indicating an orientation normal to the 001 plane. The δ(OH) bands are shown 10 times enlarged in Figure 4B. The positions of the AlAlOH, FeAlOH, and MgAlOH bending bands occur at 919, 885, and 846 cm^{-1}, respectively. The dichroic ratios of these bands are respectively 1.18, 1.13, and 1.31. The slightly different dichroic ratios indicate that the orientation of the hydroxyls depends on the nearest octahedral cations. These three δ(OH) bands are not present in the SapCa-1 spectra as Mg^{2+} is the only octahedral cation and the MgMgOH bending band at 653 cm^{-1} [30] is not visible in the ATR spectra because the cutoff of ZnSe is in the same region.

To determine band positions, intensities, and dichroic ratios, the ν(Si−O) bands were analyzed using the spectral curves shown in Figure 5. The spectra were fitted in the 1200−800 cm^{-1} region using four bands of partial Gaussian and Lorentzian character. For saponite, each of the four bands is shown offset (spectra a−d) in Figure 5 with

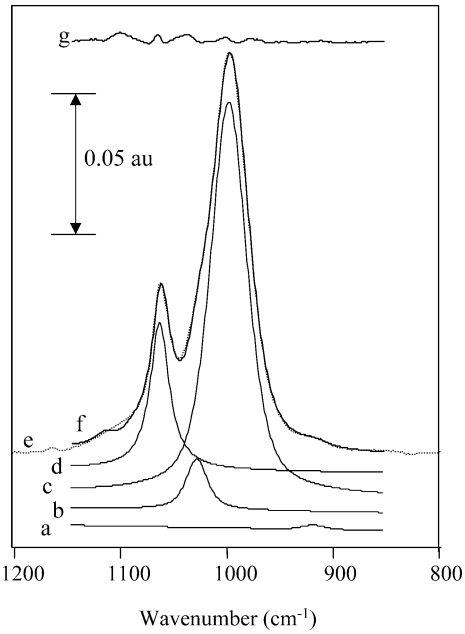

Figure 5. Curve fitting of the ν(Si−O) region. The A_p spectrum of the SapCa-THIA18 film is plotted in the 1200−800 cm^{-1} region (e), the four bands of partial Lorentzian and Gaussian character used to fit this spectra region are offset and shown by traces (a−d). The composite curve is represented by trace (f), and the residual spectrum, or the difference between the actual (e) and calculated (f) spectra, is shown at the top by trace (g).

actual (e) and synthetic composite spectra (f) overlaid. In addition, the spectral residual of the actual spectrum (e) minus the synthetic spectrum (f) is shown at the top of Figure 5 by (g). The dominant bands for saponite in the 1200−800 cm^{-1} region are the three bands at 1063, 1027, and 996 cm^{-1}. A summary of the assignments, positions, dichroic ratios, heights, and widths of the bands in the SapCa-1 and SWy-1 spectra is given in Table 1 including the average tilt angle γ calculated according to Ahn et al.,[37] where γ is the angle between the IR transition dipole moment and the normal to the surface.

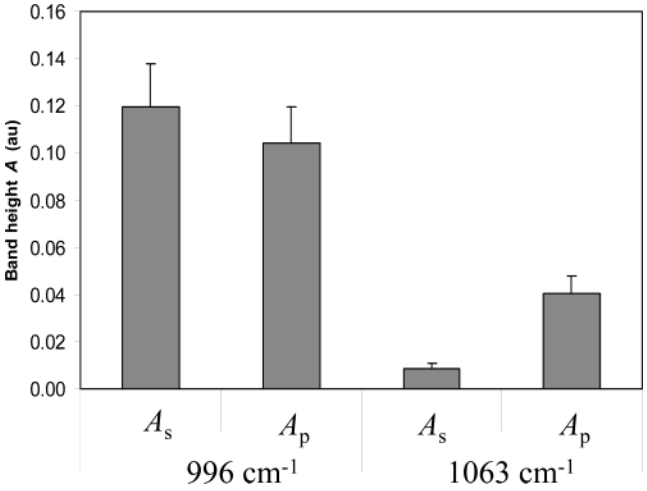

Figure 6. Band heights of the two principal ν(Si−O) bands at 996 and 1063 cm^{-1} from the s- and p-polarized ATR-FTIR spectra of the hybrid LB saponite films on ZnSe. A total of 22 hybrid LB clay films were analyzed, and the standard deviation values for each band are shown by the *y*-error bars.

The ν(Si−O) bands were not strongly influenced by the type of organic cation used to prepare the LB film. This is illustrated, in part, in Figure 6 which shows the variation in peak heights of the two dominant ν(Si−O) bands in both A_s and A_p polarizations for 22 hybrid SapCa-1 LB films prepared with five different surfactants. The strongest ν(Si−O) band at 996 cm^{-1}, for example, has an average band height of 0.12 au (±0.02). Since polarized ATR-FTIR spectra of trioctahedral smectites (i.e., saponite, hectorite, or Stevensite) have not been reported previously, it is not possible to compare the dichroic ratios with literature values. Furthermore, the bandwidths observed for the LB clay films are significantly less than those observed in prior IR studies. This is attributed to the fact that the clay films are ultrathin, corresponding to one layer of clay and highly oriented with the 001 plane of the clay parallel to the surface of the IRE such that broadening due to multiple scattering geometries and disorder is minimized.

Quantitative Analysis of ATR Spectra. The intensity of the *in-plane* ν(Si−O) band for saponite at 996 cm^{-1} and for montmorillonite at 1047 cm^{-1} of the hybrid LB films was analyzed using the model of an immobilized film in contact with a bulk rarer medium.[33] A schematic of the thin film in contact with the IRE is shown in Figure 7. In the case of a thin, weakly absorbing film, the reflectivity per internal reflection deviates only slightly from that of a nonabsorbing medium. The criteria for application of the thin film model are based on two assumptions. First, the film must be very thin. Second, the absorption coefficient $\alpha < 10^4$ cm^{-1}. For ν(Si−O), however, the α_{max} value is 3.6×10^4 cm^{-1} and this may limit the applicability of this model. Given this limitation, we apply the thin film model as a first approximation to model the intensities of the ATR-FTIR spectra.

Of particular interest in this study are the intensities of the ν(Si−O) bands as a measure of film thickness. By use of the thin film model, the ν(Si−O) band is analyzed for both ZnSe and Ge substrates, and the absorbance of a monolayer of clay is determined within the constraints of the model. The absorption coefficient of the ν(Si−O) can be determined using thick clay films in transmission where the orientation of the interacting electric field is in the plane of the clay sheets.[20] In ATR, s-polarized light has solely a *y*-component at the IRE surface that has an

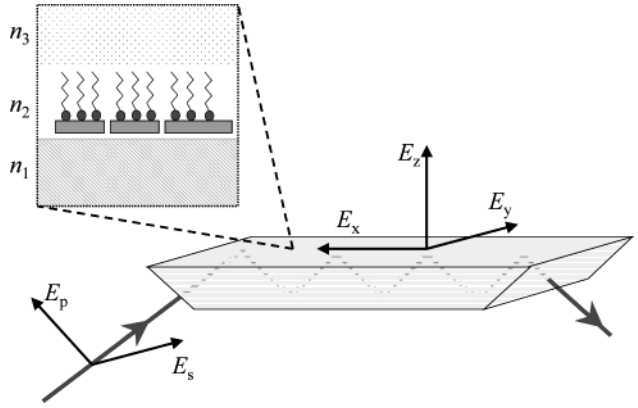

Figure 7. Schematic representation of a thin immobilized hybrid clay film of refractive index n_2 on the surface of an internal reflection element of refractive index n_1 in contact with a rarer medium (i.e., air) of index of refraction n_3. The hybrid film consists of an individual clay layer of layer thickness 0.96 nm and a cationic surfactant. When measured with s-polarized light, only the *y*-component of the IR light is present at the IRE surface. In the case of p-polarized light, the *x*- as well as the *z*-components of the electric field *E* are present.

orientation with the clay sheets similar as in transmission. This justifies the use of the absorption coefficient measured from transmission. For a single reflection, the *y*-component of the electric field amplitude in the film, $E_{y,\text{film}}$, is determined by the s-component of the electric field in the IRE, $E_{s,\text{IRE}}$, the refractive indices $n_1 = n_{\text{IRE}}$, $n_3 = n_{\text{air}}$, and the incident angle, θ, and is expressed as the ratio r_y given by

$$r_y = \frac{E_{y,\text{film}}}{E_{s,\text{IRE}}} = \frac{2\cos\theta}{(1 - n_{31}^2)^{1/2}} \quad (1)$$

where $n_{31} = n_3/n_1$. For a thin immobilized layer, the effective thickness, or interaction parameter, $d_{e,s}$ is given by

$$d_{e,s} = \frac{n_{21}\, dr_y^2}{\cos\theta} = 4\frac{n_{21}\, d\cos\theta}{(1 - n_{31}^2)} \quad (2)$$

where $n_{21} = n_2/n_1$ with $n_2 = n_{\text{film}}$. The $d_{e,s}$ parameter corresponds to a hypothetical thickness of a sample that would result in the same absorbance of a given band via transmission as obtained with the real sample thickness *d* in the ATR experiment with s-polarized light. Application of the Lambert−Beer law in ordinary transmission is given by eq 3

$$A_{\text{transmission}} = \epsilon c d \quad (3)$$

where *A* is the measured absorbance, ϵ is the molar absorptivity (cm^2 mol^{-1}), and *c* is the concentration (mol cm^{-3}). For thin films, the (ϵc) term is related to the Napierian absorption coefficient α_{max} (cm^{-1}) by eq 4[32]

$$\epsilon c = \frac{\alpha_{max}}{\ln(10)} \quad (4)$$

Application of the Lambert−Beer law to single-reflection ATR data can then be expressed by combining eqs 3 and 4

$$A_{\text{ATR,s}} = \frac{\alpha_{max} d_{e,s}}{\ln(10)} \quad (5)$$

(37) Ahn, D. J.; Franses, E. I. *J. Phys. Chem.* **1992**, *96*, 9952.

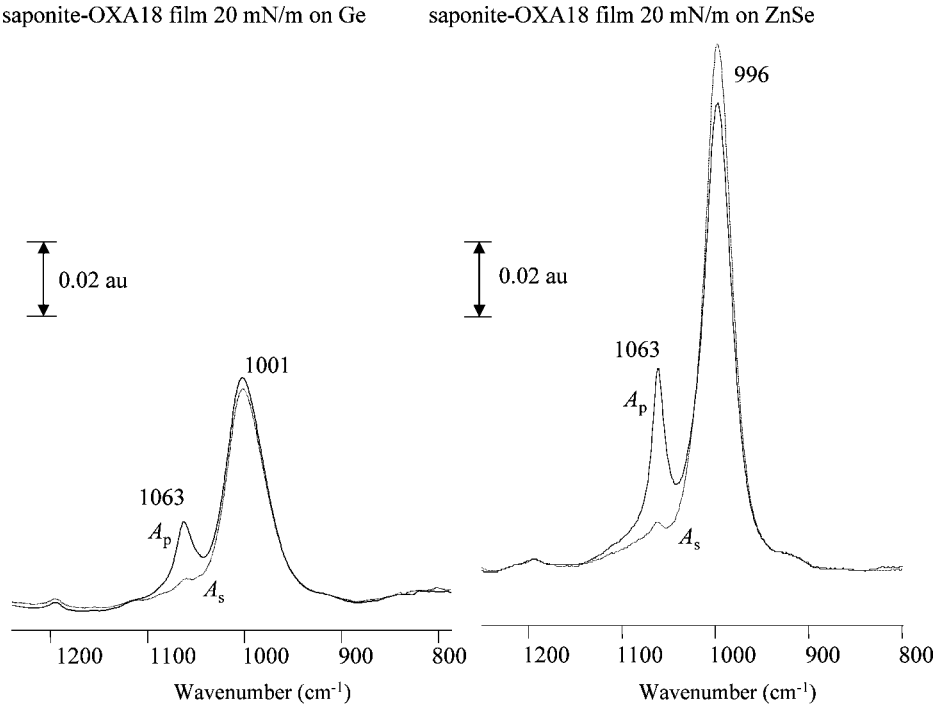

Figure 8. Comparison of polarized ATR-FTIR spectra of a SapCa-OXA18 hybrid LB film obtained at a surface pressure of 20 mN/m on Ge (left side) and ZnSe (right side) internal reflection elements. Each spectrum shares a common *y*-scale (scale bar shown).

Table 2. Comparison of Observed and Calculated s-Polarized ATR-FTIR Intensities Using the Thin-Film Approximation on ZnSe and Ge Internal Reflection Elements

	saponite (996 cm^{-1})	montmorillonite (1047 cm^{-1})
ZnSe IRE		
experimentally observed absorbance A_s of the *in-plane* ν(Si-O) band	0.10−0.14	0.082
calculated absorbance value $A_{ATR,s}$ for one 0.96 nm clay layer and optical properties listed in Table 1	0.103	0.097
Ge IRE		
experimentally observed absorbance A_s of the *in-plane* ν(Si−O) band	0.04−0.06	
calculated absorbance value $A_{ATR,s}$ for one 0.96 nm clay layer and optical properties listed in Table 1 and in text	0.054	

For multiple reflection ATR, eq 5 has to be multiplied by the number of reflections N

$$A_{ATR,s} = \frac{N\alpha_{max}d_{e,s}}{\ln(10)} \quad (6)$$

The corresponding absorbance value in ATR for s-polarization is obtained by substitution eq 2 into eq 6

$$A_{ATR,s} = 4\,\frac{Nn_{21}\,\mathrm{d}\cos(\theta)\,\alpha_{max}}{(1 - n_{31}{}^2)\ln(10)} \quad (7)$$

Hybrid LB clay films were prepared on both ZnSe and Ge internal reflection elements (IREs), and FTIR spectra are shown in Figure 8. The intensities of the polarized ATR-FTIR spectra obtained from the LB film on the ZnSE crystal were approximately twice those of the spectra obtained using the Ge IRE. In addition, the position of in-plane ν(Si−O) band was shifted slightly to a higher value on the Ge IRE crystal from 996 to 1001 cm^{-1}. The intensities of the ν(Si−O) bands obtained using the Ge IRE are significantly lower because of the higher index of refraction n_1 of Ge. This can be shown by eq 7 where the absorbance is proportional with $n_{21} = n_2/n_1$.

The predicted ATR absorbance values of a fundamental clay layer with a thickness of 0.96 nm on ZnSe and Ge IREs are compared to the experimentally observed values (Table 2). The refractive indices n of SapCa-1, SWy-1, and ZnSe at the corresponding wavelengths are shown in Table 1, $n_{Ge} = 4.004$ at 996 cm^{-1},[38] $n_{air} = 1$, $\alpha_{max\_SapCa} = 3.5 \times 10^4$ cm^{-1}, $\alpha_{max\_SWy} = 3.6 \times 10^4$ cm^{-1}.[20] Table 2 shows that the absorbance values of the hybrid LB films deposited on ZnSe and on Ge are in close agreement with the predicted IR intensity based on a single layer of clay. These data provide direct spectroscopic confirmation that single-layered hybrid clay films can be prepared using the Langmuir−Blodgett method.

Polarized Grazing Angle IRRAS-FTIR Spectra of a Hybrid Clay Film. Polarized grazing angle IRRAS spectra of a hybrid LB clay film deposited on ZnSe IRE are shown in Figure 9. The positions of the ν(Si−O) bands are in good agreement with those obtained using the ATR method. The most notable difference between these spectra and those obtained using ATR is the apparent enhancement of the apical ν(Si−O) band at 1063 cm^{-1} relative to the intensity of the in-plane ν(Si−O) band at 999 cm^{-1} in the A_p spectrum. The dichroic ratios of the 1063 and 999 cm^{-1} bands are 0.11 and 1.35, respectively. The observed polarization behavior of the IRRAS spectra is consistent with the ATR-FTIR results. The IRRAS technique is especially attractive because it can be applied to obtain

(38) Palik, E. D. *Handbook of optical constants of solids*; Academic Press: San Diego, CA, 1998.

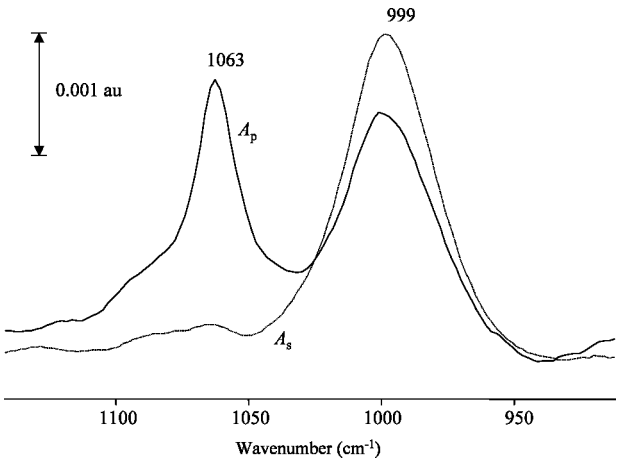

Figure 9. Polarized IRRAS spectrum of a saponite-OXA18 LB film deposited on ZnSe IRE at a surface pressure of 3 mN/m.

spectra from hybrid clay−organic monolayers directly on the air−water interface.

Conclusions

We have obtained for the first time highly resolved vibrational spectra of elementary clay layers analyzed with polarized ATR-FTIR and IRRAS-FTIR. Single layers of smectite clay mineral particles were deposited using the Langmuir−Blodgett technique on ZnSe and Ge IREs in the presence of cationic surfactant molecules. The vibrational spectra show that these layers do not contain water molecules. The out-of-plane Si−O stretching vibration shows dichroic ratios significantly different from isotropic distribution in both films containing dioctahedral and trioctahedral clay mineral particles indicating highly oriented single clay sheets. The stretching vibrations of the structural OH groups are also influenced by polarization of the light. This is in agreement with orientation of the OH groups either perpendicular to (trioctahedral clay) or more parallel with (dioctahedral clay) the plane of the elementary clay sheet. Quantitative analysis of the intensities of the Si−O stretching vibrations confirms the presence of a monolayer of single elementary clay mineral particles. AFM shows that the surface of ZnSe IRE is nearly fully covered with highly oriented single-layered clay particles.

Acknowledgment. This research is financially supported by the Fund for Scientific Research−Flanders through Grant G.0201.02 and the bilateral agreement Flanders−Hungary through Grant BIL 00/10 and partly by an IAP program on “Supramolecular Chemistry and Catalysis”. R.H.A.R. acknowledges a Ph.D. grant from IWT-Vlaanderen. C.T.J. acknowledges financial support from the U.S.D.A. National Research Initiative and a fellowship of the K.U. Leuven and travel support from WO.008.00 (Fund for Scientific Research−Flanders).

LA026786R